ACS Photonics

Article

Cite This: ACS Photonics 2018, 5, 2960−2968

Plasmonic Enhancement of Two-Photon-Excited Luminescence of Single Quantum Dots by Individual Gold Nanorods

Weichun Zhang, Martín Caldarola, Xuxing Lu, and Michel Orrit*

Huygens-Kamerlingh Onnes Laboratory, Leiden University, 2300 RA Leiden, The Netherlands

Supporting Information

ABSTRACT: Plasmonic enhancement of two-photon-excited fluorescence is not only of fundamental interest but also appealing for many bioimaging and photonic applications. The high peak intensity required for two-photon excitation may cause shape changes in plasmonic nanostructures, as well as transient plasmon broadening. Yet, in this work, we report on strong enhancement of the two-photon-excited photoluminescence of single colloidal quantum dots close to isolated chemically synthesized gold nanorods. Upon resonant excitation of the localized surface plasmon resonance, a gold nanorod can enhance the photoluminescence of a single quantum dot more than 10 000-fold. This strong enhancement arises from the combined effect of local field amplification and the competition between radiative and nonradiative decay rate enhancements, as is confirmed by time-resolved fluorescence measurements and numerical simulations.

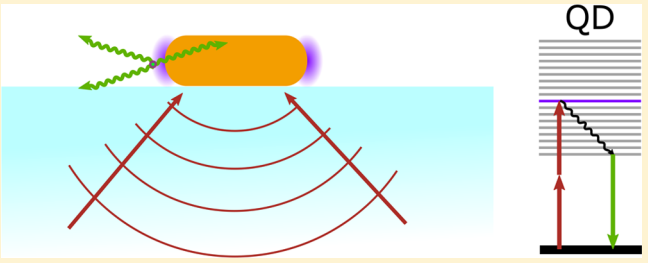

KEYWORDS: *quantum dots, two-photon-excited luminescence, plasmonic enhancement, gold nanorods*

Due to their unique properties associated with surface plasmons, nanostructures based on metal nanoparticles have been extensively studied for their potential in various applications, such as surface-enhanced Raman spectroscopy,[1,2] metal-enhanced fluorescence,[3−5] and second-harmonic generation.[6,7] Plasmonic nanostructures were found to significantly enhance the fluorescence emission of adjacent chromophores as a result of the interplay of several factors, including excitation enhancement because of the high local field, spontaneous radiative emission enhancement from resonant Purcell effect, and fluorescence quenching due to nonradiative energy transfer to the metal.[8,9]

Apart from the extensive research on the enhancement of conventional one-photon-excited fluorescence,[3,10−13] the last two decades have seen a growing interest in metal-enhanced fluorescence under two-photon excitation, which is known for the advantages of intrinsic optical sectioning, deeper penetration into biological tissues, and, under certain conditions, lower photodamage. Upon two-photon excitation, a much larger fluorescence enhancement is expected because of the quadratic dependence of two-photon absorption on the excitation intensity. Starting from the 1990s, metal-enhanced two-photon-excited fluorescence has been experimentally demonstrated with lithographically made flat or patterned metal films.[9,14,15] There have also been reports on the enhancement of upconversion luminescence using plasmonic nanoparticles.[16,17]

Wet-chemically synthesized metal nanoparticles have been exploited as important alternative structures for plasmonic enhancement.[8,10,18,19] Among many types of metallic nanoparticles, gold nanorods are the most extensively explored. Their intense electromagnetic fields associated with the narrow, strong, and tunable plasmon resonance contribute to large enhancement of the fluorescence signal of nearby fluorescent emitters such as molecules and quantum dots. Compared to metal surfaces and nanoparticle clusters,[20,21] individual gold nanorods open the study of plasmon−choromophore interactions in a more reproducible and controllable way owing to their well-defined single-crystalline structure. Compared to nanogap antennas, such as bowties, dimers, or particles on mirror, nanorods present a more open near field, which can accommodate molecules of various sizes. Moreover, gold nanorods are chemically inert and biocompatible; therefore they are particularly interesting for biotechnological applications.

A few recent reports have successfully demonstrated enhanced two-photon absorption and emission using various systems of nanocomposites composed of colloidal nanorods surrounded by fluorophores.[9,22−25] However, the enhancement factors reported in ensembles are reduced by averaging over many fluorophores, most of which are not in the best position.

Combined single-molecule and single-particle measurements are needed to bridge the gap between theory and experiments. Moreover, single-molecule and single-particle measurements have the potential of revealing the intrinsic nature of the plasmon−emitter interactions that is usually hidden in ensemble experiments by nanoparticle inhomogeneities, such as size fluctuations and local environment variations.

Received: March 7, 2018
Published: June 11, 2018

DOI: 10.1021/acsphotonics.8b00306
ACS Photonics 2018, 5, 2960−2968

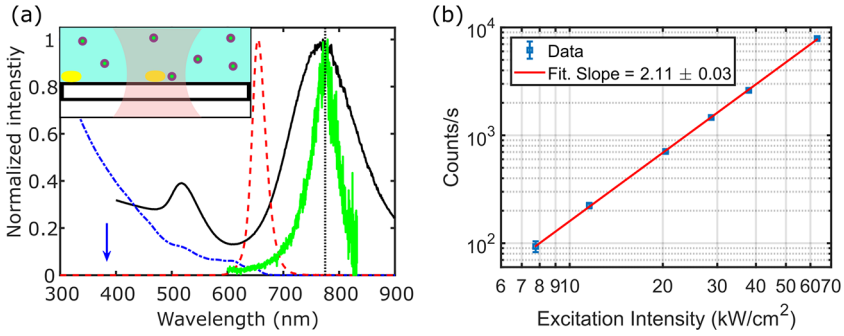

Figure 1. Quantum dot and gold nanorod optical characterization. (a) Spectra of gold nanorods and quantum dots. The black and green solid lines show the bulk extinction spectrum of gold nanorods dispersed in water and the one-photon-excited photoluminescence spectrum of an immobilized single gold nanorod, respectively. One-photon absorption and emission spectra of the quantum dots diluted in water are shown as the blue dot-dashed line and red dashed line, respectively. The vertical dotted line shows the wavelength of the Ti:sapphire laser. The blue vertical arrow indicates the wavelength corresponding to the total energy of two excitation photons. The inset shows a simplified schematic of the enhancement experiment (the yellow cylinders represent gold nanorods; core/shell circles, quantum dots). (b) Log–log plot showing the quadratic dependence of photoluminescence emission of the quantum dots on the excitation intensity. The photoluminescence emission is from a 30 nM quantum dot solution with 1 mM NaCl.

While seemingly a straightforward idea, two-photon-excited fluorescence enhancement with a single-emitter–single-nanostructure system was investigated theoretically[26] and only achieved experimentally in a very recent work by Gong et al., where the two-photon-excited luminescence intensity from single epitaxially grown InGaN quantum dots (QDs) was enhanced by a factor of 5000 using the strong field enhancement by a silver-coated pyramid structure at a temperature of 7 K.[27] Indeed, two possible major obstacles stand in the way to experimentally testing the two-photon fluorescence enhancement. First, the high peak intensities required for efficient two-photon excitation might damage the plasmonic structure, if not after a single pulse, certainly upon repeated excitation by millions of pulses over long acquisition times. Photothermal reshaping of gold nanorods under femtosecond pulses[28−30] limits the laser intensity one can use for two-photon excitation. Second, the excitation by intense femtosecond pulses tremendously heats up the electron gas by up to thousands of K, thereby broadening the plasmon resonance[31] and potentially hindering plasmonic enhancement. Added to the difficulty of a precise positioning of a single emitter with respect to the near field of plasmonic structures, these two problems may hamper plasmonic enhancement of two-photon excitation.

Our earlier studies have shown that, by exploiting the random diffusion of single molecules around single gold nanorods, the fluorescence of a low-quantum-yield dye could transiently be enhanced by 3 orders of magnitude.[8,18] Motivated by the theoretical limit to two-photon-excited fluorescence enhancement, we exploited diffusion and transient sticking of single colloidal QDs to study the strong enhancement of their two-photon-excited luminescence by single gold nanorods at room temperature. We find enhancement of two-photon-excited luminescence by more than 4 orders of magnitude for *single* QDs in the vicinity of a *single* immobilized gold nanorod at room temperature. The enhancement factor shows a clear dependence on the nanorod's surface plasmon resonance wavelength and is maximum when the resonance wavelength overlaps with the excitation laser wavelength. The achieved enhancement is in good agreement with the predictions of numerical calculations. The dependence on surface plasmon resonance (SPR) wavelength and the fair agreement with simulations show that the transient broadening of the plasmonic resonance by femtosecond excitation is not a limiting factor for two-photon-excited fluorescence enhancement by individual gold nanorods.

RESULTS AND DISCUSSION

The colloidal QDs in our study (Qdot 655 ITK amino (PEG) from Invitrogen) are CdSe/ZnS core–shell structures, which are further coated with an amphiphilic polymer shell to enable conjugation of amine-derivatized polyethylene glycol. The shape of the core-shell is rod-like with a length of ∼12 nm and a width of ∼7 nm.[32] See Supporting Information for more details about the QDs' structure. The narrow emission band centered at 655 nm is well away from the longitudinal plasmon resonance of the gold nanorods, as can be appreciated in Figure 1. This feature results in a good contrast of signal from single quantum dots against a background from the intrinsic luminescence of the gold nanorods if an appropriate bandpass filter is used. Two-photon photoluminescence was excited by a mode-locked Ti:sapphire laser operating at 76 MHz pulse repetition rate and ∼220 fs pulse width. The wavelength was set to 775 nm to efficiently excite the longitudinal plasmon resonance of the gold nanorods. More information about the optical setup can be found in the Methods section and the Supporting Information.

To determine whether the photoluminescence of QDs generated by the femtosecond laser is a result of instantaneous two-photon absorption, we measured the photoluminescence emission intensity from a diluted aqueous suspension of Qdot 655 with respect to the average intensity at the center of the focused excitation beam. Figure 1(b) plots this relation in log–log scale, yielding a slope of 2.11 ± 0.03, which confirms the two-photon excitation origin of the observed luminescence from the QDs.

Prior to the luminescence enhancement experiments, we measured the one-photon-excited photoluminescence spectra of gold nanorods immobilized on a coverslip and immersed in water. We selected single gold nanorods through their narrow and Lorentzian spectral shape for our later measurements (Supporting Information, Figure S3). Afterward, the nanorods were immersed in a 30 nM Qdot 655 solution with 3 mM NaCl (inset of Figure 1(a)). Photoluminescence photons were recorded on individual gold nanorods under the excitation of

DOI: 10.1021/acsphotonics.8b00306
ACS Photonics 2018, 5, 2960−2968

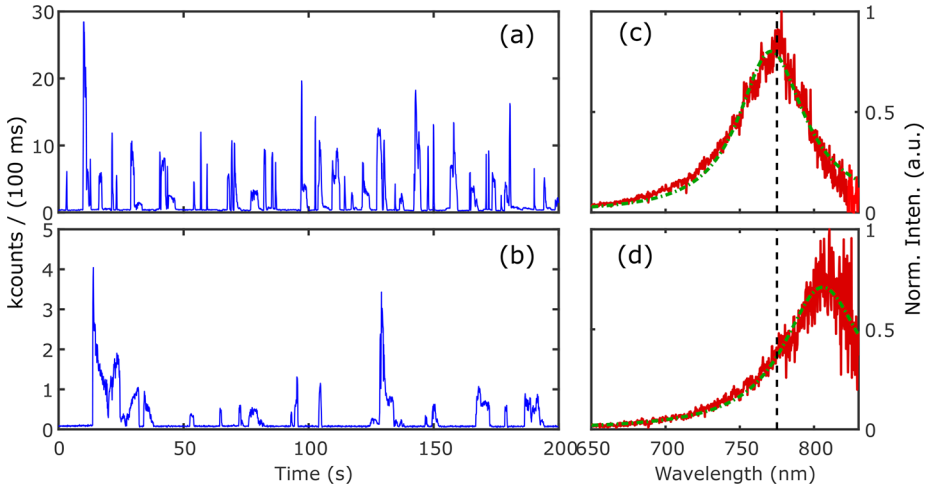

Figure 2. Enhanced two-photon-excited luminescence from single QDs. (a, b) Two-photon-excited luminescence intensity time traces (100 ms/bin) taken on two single nanorods immersed in a 30 nM QD aqueous solution with 3 mM NaCl and (c, d) the corresponding one-photon-excited luminescence spectra of the nanorods measured in water. The excitation intensity at the center of the two-photon excitation volume was 1.55 kW/cm^2 (circularly polarized). The one-photon-excited spectra show a narrow Lorentzian line shape (green dashed lines), confirming that they are from single nanorods. The low near-infrared response of the optics including the spectrometer CCD is responsible for the high noise. The wavelength of the laser (775 nm) is also shown as the dashed vertical lines in (c) and (d).

the femtosecond laser with an average excitation intensity of 1.55 kW/cm^2 (1 μW at the objective focus) at the center of the focused excitation volume. We note that this intensity is well below that required for photothermal reshaping of a single gold nanorod with a low number (~1 to 10^4) of ultrafast pulses.[28−30] Indeed, we did not observe any luminescence intensity change from the gold nanorods upon femtosecond irradiation, even after our extended measurements of several minutes. Moreover, the measured one-photon-excited photoluminescence spectra of gold nanorods before and after femtosecond irradiation showed no noticeable shift or changes. Therefore, the nanorods were not reshaped during our measurements. It is worth mentioning that most previous studies on ultrafast reshaping of gold nanoparticles were done with single or a few pulses. Under extended pulsed irradiation, however, cumulative surface diffusion of gold atoms leads to a much lower reshaping threshold in terms of average power. Indeed, we started to observe reshaping for some nanorods with an excitation power of ≥3 μW (intensity of 4.7 kW/cm^2 with circular polarization).

Figure 2 shows two typical intensity traces (binned to 100 ms) from two gold nanorods whose spectra are shown in the right panels. The spectra have been corrected for the spectral response of the optical setup (see Figure S3). Intensity bursts are observed for both nanorods, which we attribute to gold-nanorod-enhanced photoluminescence emission of single QDs. Some weak background signal comes mostly from the two- and multiphoton-excited luminescence of the gold nanorods.[33] Note that the bursts shown in Figure 2 last generally a few tens of milliseconds to a few seconds.

We used two-photon-excited fluorescence correlation spectroscopy with a twofold purpose: first, to obtain the diffusion time of our QDs in the confocal volume and, second, to measure the single-QD brightness, needed to quantify the enhancement factor.

The diffusion time of a single QD in the near field of a rod is shorter than one microsecond, estimated from the diffusion time in the confocal volume, measured by autocorrelating the two-photon-excited luminescence of freely diffusing QDs (Figure S4). Thus, we attribute the bursts to transient sticking of QDs onto the substrate and/or the gold nanorods (note that the emitting part of a QD is separated from the gold surface by the polymer coating, therefore sticking to a gold nanorod does not necessarily completely quench its photoluminescence). This nonspecific sticking effect was found in a few studies to be strongly dependent on the properties of the diffuser and the surrounding medium as well as the surface conditions of the metal and substrate.[18,34,35] In our case, the addition of a proper amount of NaCl to the QD solution was essential for transient sticking and, hence, for observing luminescence bursts. If no NaCl was added, we saw only luminescence from gold nanorods. On the other hand, when the NaCl concentration was too high, the bursts were too long to be separated from each other (data shown in Supporting Information Figure S11).

From the correlation measurements explained in detail in the Supporting Information, we obtained an average unenhanced single-QD brightness of 1900 ± 70 counts/s at 15.5 kW/cm^2 illumination intensity. We note here that this is an ensemble-averaged result that may show significant fluctuations when compared to single-QD data due to variations from dot to dot, for example in size. We also note that the intensity used for this unenhanced measurement is 10 times higher than the intensity used for the enhancement experiment on a nanorod.

We attribute the large difference in burst intensities recorded on the same gold nanorod to the random locations and orientations of the QDs with respect to the gold nanorod. Additionally, the size distribution of the QDs in our sample contributes further to the intensity inhomogeneity of the enhancement bursts. We observed that the more intense the bursts are, the shorter they last, as can be seen in Figure 2. Indeed we confirmed this behavior by plotting the burst duration as a function of the burst detected intensity for an enhanced time trace (see Supporting Information Figure S9). In addition, we note that we did not observe characteristic luminescence blinking of QDs.[36,37] However, blinking may occur either on a time scale shorter than our resolution or at

DOI: 10.1021/acsphotonics.8b00306
ACS Photonics 2018, 5, 2960−2968

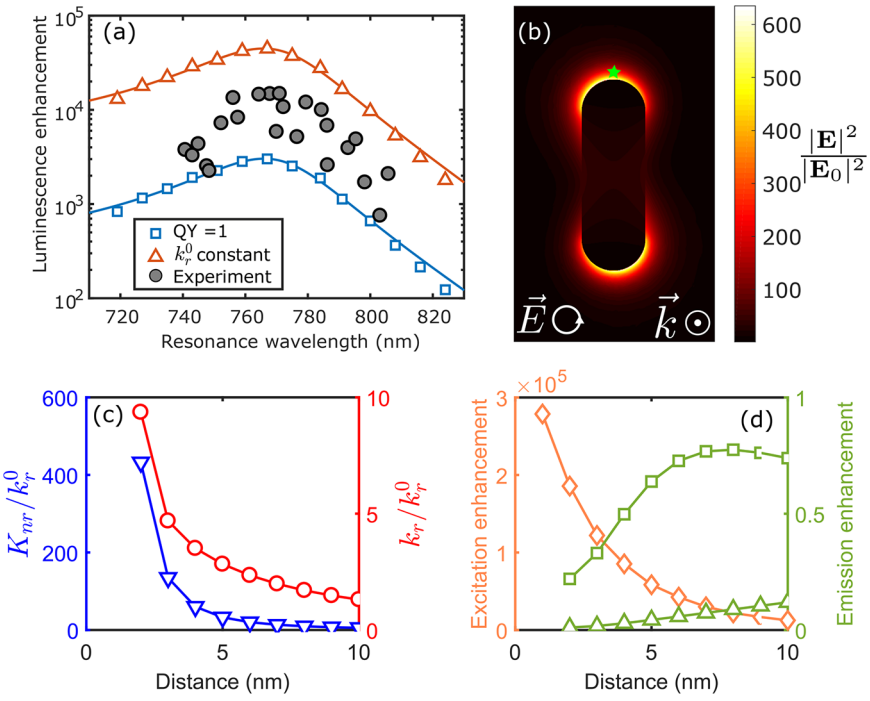

Figure 3. Enhancement dependence on plasmon resonance. (a) Measured maximum two-photon-excited luminescence enhancement factors for 23 gold nanorods plotted against their plasmon resonance wavelengths are shown as gray circles. The numerically calculated overall enhancement factors for two different models of QD luminescence (see text) are shown as red triangles and blue squares. Solid lines are guides to the eye. For the calculations, the emitter is assumed to be located 5 nm away from the tip of the nanorod (green star in (b)). (b) Calculated near-field intensity map of a 38 nm × 114 nm nanorod in water (surface plasmon resonance at 775 nm), excited with circularly polarized light. The wavevector direction is indicated as $\vec{k}$. (c) Calculated radiative rate enhancement (k_r/k_r^0, red circles, right axis) and relative additional nonradiative rate (K_{nr}/k_r^0, blue triangles, left axis) of a QD as a function of the distance to the tip of the nanorod. (d) Calculated excitation enhancement (orange diamonds) and emission enhancement (green squares and triangles) as functions of the distance to the tip of the nanorod. The squares and triangles correspond to the two models mentioned above for (a). The excitation wavelength was 775 nm (circularly polarized) for both experiments and simulations.

times longer than the burst duration. We note that earlier observations indicate that QD blinking is greatly suppressed when coupled to plasmonic structures.[38,39]

Blank experiments were performed to verify that the bursts are from gold-nanorod-enhanced single QDs. We recorded time traces on a area without a nanorod under the same experimental conditions. We also measured single nanorods with the same excitation but immersed in 3 mM NaCl without QDs. In both cases, we never observed any burst, as shown in the example traces in the Suppporting Information (Figure S5). Moreover, we recorded time traces on *the same* single gold nanorod in solutions with different concentrations of QDs (6 and 30 nM). We found higher occurrence of bursts in the solution with higher QD concentration (Figure S6), which clearly demonstrates the linear dependence of burst frequency on QD concentration.

The previous experiments convinced us that the bursts stem from enhanced two-photon-excited luminescence of single QDs. The size of the QDs is as large as the near field, so it is unlikely that more than one QD resides in the near field. We have to consider the possibility of aggregates of QDs, as we did find evidence of them (Figure S4) with an occurrence of 20 per 300 s in the confocal volume. However, considering a near-field volume that is ~2000 times smaller than the confocal volume (V_{conf} = 3 × 10^{-2} fL, V_{NF} = 1.4 × 10^{-5} fL), the probability of seeing one QD aggregate in the near-field in a measuring time of 300 s is only 1%.

In order to calculate the luminescence enhancement factor, we need to compare the two-photon-excited enhanced intensity with the unenhanced brightness of a single quantum dot (i.e., count rate per dot). The former can be extracted from the time traces in Figure 2, and the latter was obtained using two-photon fluorescence correlation spectroscopy (FCS).[40] The same QD solution used for the enhancement experiment was excited with an average excitation intensity of 15.5 kW/cm^2 (below saturation). By scaling with the quadratic power dependence of two-photon-excited luminescence, we found the count rate per dot to be 19.0 ± 0.1 counts/s at an excitation intensity of 1.55 kW/cm^2. See the Supporting Information (Figure S4) for details. The maximum intensity of the burst shown in Figure 2(a) is 2.84 × 10^2 kcounts/s for circularly polarized excitation. It is from a single QD enhanced by the nanorod against a background signal of 2850 counts/s from the nanorod and other QDs in the focal volume. On the basis of an average brightness of 19.0 counts/s per QD measured with FCS at the same excitation intensity, we calculate an enhancement factor of 1.5 × 10^4 for circularly polarized light. We used circularly polarized light to excite all the nanorods in the glass surface, regardless of their orientation. If we would use linearly polarized light parallel to the long axis of the nanorod, we expect to observe a larger enhancement of 6 × 10^4.

We would like to emphasize that the reported enhancement factor comes from looking at the highest burst in a time trace, as is commonly done in the literature. However, there are other alternative methods to obtain the enhancement factor from the same type of experimental data, leading to similar results.[41]

DOI: 10.1021/acsphotonics.8b00306
ACS Photonics 2018, 5, 2960−2968

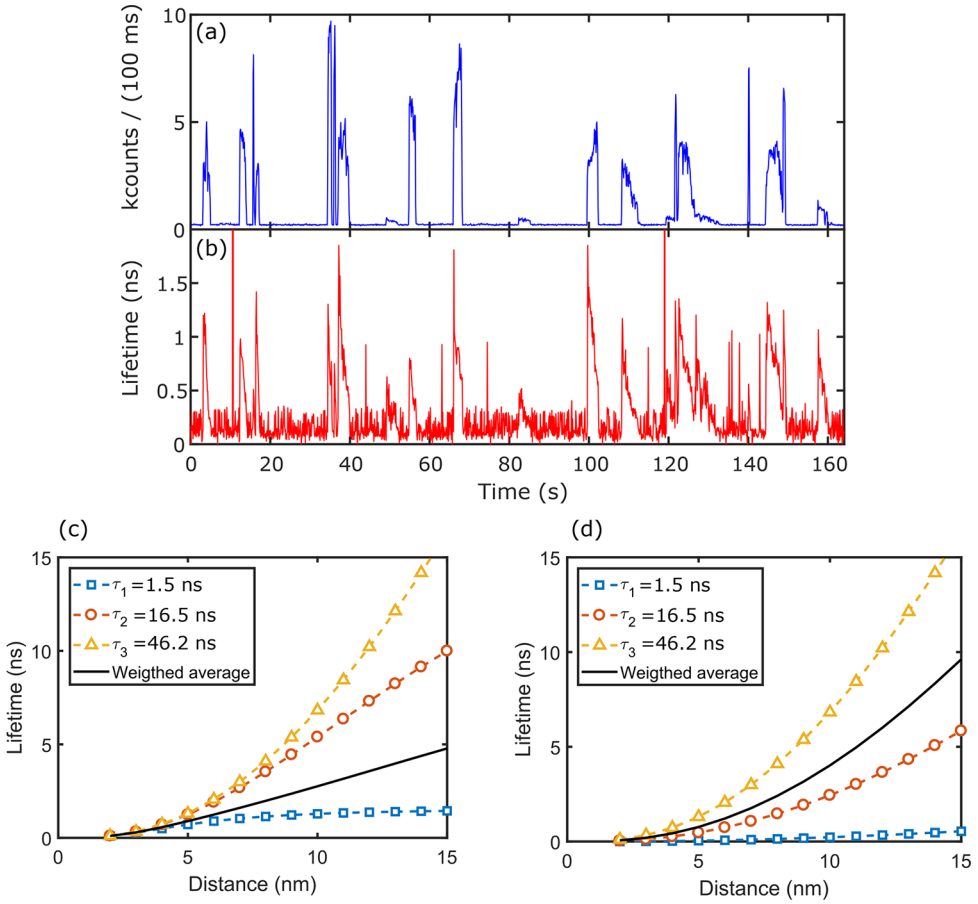

Figure 4. QDs enhanced photoluminescence lifetime. (a) Photoluminescence intensity trace and the corresponding lifetime trace (b) measured on a single gold nanorod. (c, d) Calculated lifetime of a QD as a function of the distance to the tip of the nanorod, with different lifetimes indicated in the legend. For the calculation, the size of the single nanorod is 38 nm × 114 nm with a plasmon resonance of 775 nm in water, corresponding to the maximum enhancement. For (c) we assumed a constant radiative rate for all the species with a unity quantum yield for the longest component (τ_3). For (d) we assumed a unit quantum yield for all the species.

Comparison of Figure 2(a) and (b) clearly reveals that the enhancement strongly depends on the longitudinal plasmon resonance wavelength of the gold nanorod. The plasmon resonance of the nanorod shown in the upper panel matches the laser wavelength very well, giving rise to almost 1 order of magnitude more intense bursts than the other nanorod, whose resonance wavelength is ∼30 nm away from the laser wavelength. We repeated the measurements on 23 different individual nanorods and plotted their maximum luminescence enhancement factors in Figure 3(a). The strongest enhancement was achieved by a nanorod with a surface plasmon resonance wavelength of 771 nm. The time trace and spectrum of this nanorod are those shown in Figure 2(a). We note that our observation of two-photon-excited enhanced emission gives evidence that the transient plasmon broadening is no serious limitation to the two-photon enhancement.

To understand the measured luminescence enhancement theoretically, we employed a finite-element method (Comsol Multiphysics) and a boundary element method to model the quantum dot−nanorod system. The photoluminescence emission of an emitter in the vicinity of a gold nanorod is altered through the modification of both the excitation and emission rates, as illustrated by Khatua et al. considering a two-level model.[8] For excitation intensities below saturation, we can treat absorption and emission independently. This assumption is justified because the saturation intensity is ∼2000 times higher than the incident laser intensity in our enhancement experiments (Figure S8). Such a high saturation intensity is well above the local field intensity that can be attained by the nanorods used in our study, about 300 times larger than the incident intensity (see Figure 3(b)). Therefore, the overall enhancement factor is approximated by the product of excitation enhancement and emission enhancement.[8] See the Methods section for the details of the simulations.

In Figure 3(a), along with measured photoluminescence enhancement factors, we plot the calculated overall enhancement factors for point emitters that are 5 nm away from the tip of the nanorod as a function of the plasmon resonance wavelength of the nanorod, while the near-field intensity map of the nanorod with the highest enhancement is shown in Figure 3(b). From this map, it is straightforward to obtain the excitation enhancement as $E_{ex} = (I/I_0)^2$, which is shown in panel (d), left axis, as a function of the distance to the tip.

In Figure 3(c) we plot the calculated radiative rate enhancement (k_r/k_r^0, blue triangles) and relative additional nonradiative rate (K_{nr}/k_r^0, red circles) of a QD against the distance to the tip of a single nanorod. The size of the nanorod in the calculation was 38 nm × 114 nm with a plasmon resonance of 775 nm in water. The high additional nonradiative rate due to the strong absorption of the gold nanorod (quenching) leads to an emission "enhancement" factor that is lower than unity.

DOI: 10.1021/acsphotonics.8b00306
ACS Photonics 2018, 5, 2960−2968

The emission enhancement is proportional to the inverse of the emitter's intrinsic quantum yield (see Methods), which is not a priori known in our experiments. First, the quantum yield of individual QDs varies due to the size distribution.[32] Second, it is known that the quantum yield of a single QD fluctuates with time in a manner that is strongly correlated with the luminescence lifetime.[42−45] Moreover, the presence of on−off blinking and intermediate states[43] adds further complications to the "on-state" quantum yield of a QD.

In addition to these unknown parameters of the system, we modeled the measured luminescescence decay with three exponential components (see Supporting Information Figure S7 for details) for unenhanced QDs in solution. The obtained lifetimes are τ_1 = 1.5 ns, τ_2 = 16.5 ns, and τ_3 = 46.2 ns. In the absence of detailed information on the QD emission we used two simple models to calculate the emission enhancement. Model 1 assumes that the three components have the same radiative rate k_r^0. We then use the measured decay components to obtain the quantum yield for each component. We additionally assumed a unity quantum yield for the longest component. Model 2 assumes unity quantum yield for all three components. In both cases we calculated the emission enhancement for each component individually and then averaged the results with the weights obtained from the lifetime fit shown in the Supporting Information. The results for the two models are plotted in Figure 3(a) as a function of the SPR (model 1 as red triangles and model 2 as blue squares) and Figure 3(d) as a function of the gold nanorod−QD distance (model 1 as triangles and model 2 as squares). From Figure 3(a) we see that these two extreme models reproduce the resonance wavelength dependence quite well. The experimental points lie between the two curves, showing that these simple models do not give a complete quantitative description of the system. Figure 3(d) shows the calculated two-photon excitation enhancement and emission enhancement as functions of the distance to the tip of the nanorod. Overall, our experimental results agree well with theoretical calculations for both the enhancement factors and the dependence on the resonance wavelength. Therefore, comparison to theory indicates that transient plasmon broadening, if at all present, does not significantly reduce the two-photon-excited fluorescence enhancement.

It is also of interest to investigate the impact of gold nanorods on the photoluminescence lifetime of QDs. The intrinsic two-photon-excited photoluminescence lifetime of the QDs could not be accurately measured with our current system due to the high repetition rate of the Ti:sapphire laser. We noticed that it was reported that the photoluminescence lifetimes of CdSe quantum dots under one- and two-photon excitations are nearly identical.[46] Therefore, we measured the complete photoluminescece decay of the same QD solution with one-photon excitation by using a pulsed picosecond diode laser (Power Technology, Little Rock) with a repetition rate of 1 MHz and a wavelength of 635 nm, and we obtained a nonexponential decay with an average lifetime of 5.09 ns (see Supporting Information for more explanation and Figure S7 for the curve). In the presence of nanorods, we obtained the lifetimes of the enhanced two-photon-excited luminescence from the recorded time-tagged single-photon data. The instrument response function was measured by recording luminescence photons from a nanorod in the same spectral range as the QDs.[33] For each time bin of 100 ms, we recorded a luminescence decay histogram and, after deconvoluting the instrument response function, fitted it with a single-exponential function and plotted the temporal evolution of the lifetimes (i.e., a lifetime trace) in Figure 4(b). The corresponding photoluminescence intensity trace from the same nanorod is plotted as well in Figure 4(a) for comparison. We observed a shortened lifetime smaller than 2 ns due to the presence of the nanorod.

We also calculated numerically the photoluminescence lifetime for a QD near the gold nanorod for the three components using the simple model mentioned before. Figure 4(c,d) show the expected lifetime for each component and the weighted average result for the two models presented before. In both cases, the weighted average lifetime for a QD in the vicinity of the gold nanorods is below 5 ns, in agreement with the observed shortened lifetime. This strong shortening of lifetime is a combination of an enhanced radiative decay rate (k_r) and the additional nonradiative decay pathways due to the dissipation of gold (k_{nr}). The relation between luminescence intensity and lifetime is complicated due to the interplay between electromagnetic intensity enhancement and changes of radiative and nonradiative decay rates.

Interestingly, we systematically found many photoluminescence bursts that show nearly constant or even increasing intensities but shorter lifetimes. We speculate that this interesting behavior may be a result of some photochemistry that is happening to the QDs in the vicinity of the nanorods. Oxidation of the QDs is unlikely the cause, as we observed the same phenomenon after removing oxygen by saturating the sample solution with argon gas (data not shown). With the current set of data and experimental design, we are not able to identify the underlying mechanism. Obviously, the emission intensity and decay rates are strongly dependent on the QD location with respect to the nanorod, which is not a priori known in our case. Further investigations, preferably single-emitter and single-particle studies with well-defined structures and positions, are required to clarify this point.

CONCLUSIONS

In summary, this work demonstrates the enhancement of two-photon-excited luminescence from single emitters by wet-chemically synthesized single gold nanorods. Quantum dots with high two-photon brightness are used to detect enough luminescence signal while maintaining the shape of gold nanorods by using very low excitation intensity. An enhancement factor of 15,000 (60,000 with linearly polarized light parallel to the long direction of the nanorod) is achieved by matching the plasmon resonance of a gold nanorod with the excitation wavelength. This large enhancement results from the plasmon resonance-enhanced strong near field at the tips of the gold nanorods and the quadratic dependence of two-photon absorption and the excitation intensity. We also observed a significant change in the quantum dot's luminescence lifetime due to interaction with the nanorods.

The good agreement between our experimental results and simulations suggests that luminescence enhancement is not notably affected by the plasmon broadening due to the presence of high electronic temperatures. We believe this study sheds some light on metal-enhanced fluorescence and paves the way for future studies of single-molecule−single-particle plasmonic enhancement of two-photon-excited luminescence. The luminescence enhancement by gold nanorods will be valuable for two-photon fluorescence applications,[9,23] espe-

DOI: 10.1021/acsphotonics.8b00306
ACS Photonics 2018, 5, 2960−2968

cially when a low excitation power is required by experimental conditions.

METHODS

Gold Nanorods. Aqueous suspensions of cetyltrimethylammonium bromide (CTAB)-stabilized gold nanorods were purchased from Nanopartz Inc. (A12-40-780-CTAB). The average size was 38 nm × 118 nm by diameter and length. Individual isolated gold nanorods (GNRs) were immobilized onto a glass coverslip by spin coating suspensions with reduced CTAB concentration.[18] No interactions between GNRs are expected because of the long interparticle distance (>1 μm). After spin coating we removed the stabilization ligands from the surface of the gold nanorods by ozone treatment for 30 min. This results in bare gold nanorods (i.e., without any ligands in their surface), allowing easy access for the quantum dots. A typical multiphoton luminescence image of the immobilized nanorods is shown in Figure S2.

Two-Photon Microscopy. We performed two-photon-excited luminescescence measurements on a home-built sample-scanning fluorescence microscope system. The glass coverslip with deposited gold nanorods was immersed in a dilute aqueous solution of QDs. A mode-locked Ti:sapphire laser (Coherent Mira 900) was used as the two-photon excitation source, operating at 775 nm, 76 MHz pulse repetition rate, and ∼220 fs pulse width. The excitation power was measured at the output of the objective. Circular polarization was used, as it excites all the GNRs irrespective of their random orientation in the focal plane. Time-resolved photoluminescence photons from QDs and gold nanorods were recorded with an avalanche photodiode using appropriate detection filters and processed with a time-correlated single photon counting card (TimeHarp 200, PicoQuant GmbH). A 532 nm continuous wave laser and a spectrometer equipped with a liquid-nitrogen-cooled CCD (Acton SP-500i, Princeton Instruments) were used to measure the one-photon-excited luminescence spectrum of each nanorod, which was shown previously[47] to closely resemble its scattering spectrum. Spectra of nanorods were measured in water without QDs prior to the enhancement measurements. Only single nanorods evidenced by their narrow Lorentzian spectral lineshapes were considered in this study. See the Supporting Information (Figure S1) for a more complete description of the optical setup.

Enhancement Factor Simulations. The excitation enhancement was calculated with a finite-element method using Comsol Multiphysics. The near-field intensity maps of single gold nanorods with resonance wavelengths ranging from 711 to 824 nm in water were calculated. The resonance wavelengths were tuned by changing the length while keeping a constant diameter of 38 nm. The dielectric permittivity for gold was taken from Johnson and Christy,[48] and the refractive index of the ambient medium was taken as 1.33. The theoretical excitation enhancement E_{exc} for two-photon absorption is the squared ratio of local field intensities with and without the nanorod, $E_{exc} = I^2/I_0^2$, at the emitter's position.

We used a boundary element method (SCUFF-EM) to evaluate the modifications of decay rates and emission enhancement using a classical electrodynamics approach.[49,50] For simplicity, a QD was modeled as a radiating point dipole ($\mathbf{p}_0$) oscillating at a frequency of ω, which corresponds to the emission wavelength of the QD.

The time-average power radiated by a QD in a medium is

$$P_{r0}(\omega) = \frac{|\mathbf{p}_0|^2}{4\pi\varepsilon_0}\frac{n\omega^4}{3c^3}$$

where n is the relative index of the medium, c is the speed of light, and ε_0 is the vacuum permittivity. In the vicinity of a nanoantenna, however, both the radiative and nonradiative decay rates are modulated by coupling to the plasmonic modes. The radiative rate enhancement factor (E_{rad}) due to resonant Purcell enhancement can be calculated as the ratio of the total radiated power by the emitter−antenna system (P_{rad}) and the power radiated by an isolated emitter (P_{r0}):

$$E_{rad} = k_r/k_r^0 = P_{rad}/P_{r0}$$

where k_r and k_r^0 are the radiative decay rates with and without the antenna, respectively. Likewise, the additional nonradiative rate (K_{nr}) due to the dissipative losses inside the metal is derived from the power absorbed by the nanorod (P_{abs}):

$$K_{nr}/k_r^0 = P_{abs}/P_{r0}$$

In the simulation, P_{abs} was calculated by integrating the time-averaged Poynting flux over the nanorod surface, which was modeled as a spherically capped cylinder. The sum of P_{rad} and P_{abs} was calculated as[S1]

$$P_{rad}(\omega) + P_{abs}(\omega) = \frac{\omega^3}{2c^2\varepsilon_0}|\mathbf{p}_0|^2[\mathbf{n}\cdot\mathrm{Im}[\mathbf{G}(\mathbf{r}, \mathbf{r}; \omega)]\cdot\mathbf{n}]$$

where $\mathbf{G}(\mathbf{r}, \mathbf{r}; \omega)$ is the Green tensor at the emitter's position $\mathbf{r}$ and $\mathbf{n}$ is the unit vector in the direction of the dipole moment. The emission enhancement factor can be written as

$$E_{em} = \frac{\eta}{\eta_0} = \frac{E_{rad}}{\eta_0(E_{rad} + K_{nr}/k_r^0 + 1/\eta_0 - 1)} \approx \frac{E_{rad}}{\eta_0(E_{rad} + K_{nr}/k_r^0)}$$

where η and η_0 are the quantum yield of the emitter with and without the antenna, respectively. E_{em} is proportional to the inverse of the emitter's intrinsic quantum yield for a given emitter−antenna configuration, but independent of its intrinsic lifetime. Due to emission enhancement, the luminescence lifetime of the emitter is shortened:

$$\tau/\tau_0 = \eta_0^{-1}(E_{rad} + K_{nr}/k_r^0 + 1/\eta_0 - 1)^{-1} \approx \eta_0^{-1}(E_{rad} + K_{nr}/k_r^0)^{-1}$$

In the calculation of E_{rad} and K_{nr}, it was assumed that the point dipole is placed along the long axis of the nanorod with a certain distance from the tip, and all the results were averaged over the actual luminescence spectrum of the QD. Unlike a fluorescent molecule, an elongated QD has three dipolar axes, where two are degenerated. Therefore, we simulated both orientations, parallel (∥) and perpendicular (⊥) and averaged the results using 1/3(∥+2 ⊥).

We modeled the three components with lifetimes τ_i (i = 1, 2, 3) independently using the above approach and then averaged the results using the weights w_i obtained from the fit of the natural lifetime decay (see Supporting Information, Figure S7). We used two extreme models to assign the quantum yield of each component. In model 1 we assume that the radiative rate of all the components is the same, and we assigned a unity

DOI: 10.1021/acsphotonics.8b00306
ACS Photonics 2018, 5, 2960−2968

quantum yield to the longest component. In model 2 we assigned a unity quantum yield to the three components.

■ ASSOCIATED CONTENT

Supporting Information

The Supporting Information is available free of charge on the ACS Publications website at DOI: 10.1021/acsphotonics.8b00306.

Schematic of the experimental setup; photoluminescence (PL) image of nanorods; relative detection efficiency of the setup and corrected PL spectra of nanorods; two-photon-excited fluorescence correlation spectroscopy; blank experiments; QD concentration dependence; one-photon-excited luminescence decay of Qdot 655; excitation saturation, burst analysis: correlation between duration and intensity; quantum dot structure; enhancement time traces at different NaCl concentrations; effect of finite size of the QD (PDF)

■ AUTHOR INFORMATION

Corresponding Author

*E-mail: orrit@physics.leidenuniv.nl.

ORCID

Martín Caldarola: 0000-0001-8086-2580

Michel Orrit: 0000-0002-3607-3426

Notes

The authors declare no competing financial interest.

■ ACKNOWLEDGMENTS

The authors acknowledge financial support from NWO, The Netherlands Organization for Scientific Research (grant ECHO 712.013.003). W.Z. and X.L. acknowledge a Ph.D. grant from the China Scholarship Council. The authors thank Dr. Pedro Miguel Neves Ribeiro Paulo for his advice on the simulations.

■ REFERENCES

(1) Kneipp, K.; Kneipp, H.; Itzkan, I.; Dasari, R. R.; Feld, M. S. Ultrasensitive chemical analysis by Raman spectroscopy. *Chem. Rev.* **1999**, *99*, 2957−2976.

(2) Li, J. F.; Huang, Y. F.; Ding, Y.; Yang, Z. L.; Li, S. B.; Zhou, X. S.; Fan, F. R.; Zhang, W.; Zhou, Z. Y.; Wu, D. Y.; Ren, B.; Wang, Z. L.; Tian, Z. Q. Shell-isolated nanoparticle-enhanced Raman spectroscopy. *Nature* **2010**, *464*, 392.

(3) Bardhan, R.; Grady, N. K.; Cole, J. R.; Joshi, A.; Halas, N. J. Fluorescence enhancement by Au nanostructures: nanoshells and nanorods. *ACS Nano* **2009**, *3*, 744−752.

(4) Muskens, O. L.; Giannini, V.; Sanchez-Gil, J. A.; Gomez Rivas, J. Strong enhancement of the radiative decay rate of emitters by single plasmonic nanoantennas. *Nano Lett.* **2007**, *7*, 2871−5.

(5) Tam, F.; Goodrich, G. P.; Johnson, B. R.; Halas, N. J. Plasmonic Enhancement of Molecular Fluorescence. *Nano Lett.* **2007**, *7*, 496−501.

(6) Boyd, G.; Rasing, T.; Leite, J.; Shen, Y. Local-field enhancement on rough surfaces of metals, semimetals, and semiconductors with the use of optical second-harmonic generation. *Phys. Rev. B: Condens. Matter Mater. Phys.* **1984**, *30*, 519.

(7) Bouhelier, A.; Beversluis, M.; Hartschuh, A.; Novotny, L. Near-field second-harmonic generation induced by local field enhancement. *Phys. Rev. Lett.* **2003**, *90*, 013903.

(8) Khatua, S.; Paulo, P. M. R.; Yuan, H.; Gupta, A.; Zijlstra, P.; Orrit, M. Resonant Plasmonic Enhancement of Single-Molecule Fluorescence by Individual Gold Nanorods. *ACS Nano* **2014**, *8*, 4440−4449.

(9) Li, X.; Kao, F.-J.; Chuang, C.-C.; He, S. Enhancing fluorescence of quantum dots by silica-coated gold nanorods under one- and two-photon excitation. *Opt. Express* **2010**, *18*, 11335−11346.

(10) Fu, Y.; Zhang, J.; Lakowicz, J. R. Plasmon-Enhanced Fluorescence from Single Fluorophores End-Linked to Gold Nanorods. *J. Am. Chem. Soc.* **2010**, *132*, 5540−5541.

(11) Yang, Z.; Ni, W.; Kou, X.; Zhang, S.; Sun, Z.; Sun, L.-D.; Wang, J.; Yan, C.-H. Incorporation of Gold Nanorods and Their Enhancement of Fluorescence in Mesostructured Silica Thin Films. *J. Phys. Chem. C* **2008**, *112*, 18895−18903.

(12) Farahani, J. N.; Pohl, D. W.; Eisler, H.-J.; Hecht, B. Single quantum dot coupled to a scanning optical antenna: a tunable superemitter. *Phys. Rev. Lett.* **2005**, *95*, 017402.

(13) Kinkhabwala, A.; Yu, Z.; Fan, S.; Avlasevich, Y.; Müllen, K.; Moerner, W. Large single-molecule fluorescence enhancements produced by a bowtie nanoantenna. *Nat. Photonics* **2009**, *3*, 654.

(14) Kano, H.; Kawata, S. Two-photon-excited fluorescence enhanced by a surface plasmon. *Opt. Lett.* **1996**, *21*, 1848−1850.

(15) Jung, J.-M.; Yoo, H.-W.; Stellacci, F.; Jung, H.-T. Two-Photon Excited Fluorescence Enhancement for Ultrasensitive DNA Detection on Large-Area Gold Nanopatterns. *Adv. Mater.* **2010**, *22*, 2542−2546.

(16) Greybush, N. J.; Saboktakin, M.; Ye, X.; Della Giovampaola, C.; Oh, S. J.; Berry, N. E.; Engheta, N.; Murray, C. B.; Kagan, C. R. Plasmon-enhanced upconversion luminescence in single nanophosphor-nanorod heterodimers formed through template-assisted self-assembly. *ACS Nano* **2014**, *8*, 9482−9491.

(17) Xue, Y.; Ding, C.; Rong, Y.; Ma, Q.; Pan, C.; Wu, E.; Wu, B.; Zeng, H. Tuning Plasmonic Enhancement of Single Nanocrystal Upconversion Luminescence by Varying Gold Nanorod Diameter. *Small* **2017**, *13*, 1701155.

(18) Yuan, H.; Khatua, S.; Zijlstra, P.; Yorulmaz, M.; Orrit, M. Thousand-fold enhancement of single-molecule fluorescence near a single gold nanorod. *Angew. Chem., Int. Ed.* **2013**, *52*, 1217−21.

(19) Samanta, A.; Zhou, Y.; Zou, S.; Yan, H.; Liu, Y. Fluorescence quenching of quantum dots by gold nanoparticles: a potential long range spectroscopic ruler. *Nano Lett.* **2014**, *14*, 5052−7.

(20) Wenseleers, W.; Stellacci, F.; Meyer-Friedrichsen, T.; Mangel, T.; Bauer, C. A.; Pond, S. J.; Marder, S. R.; Perry, J. W. Five orders-of-magnitude enhancement of two-photon absorption for dyes on silver nanoparticle fractal clusters. *J. Phys. Chem. B* **2002**, *106*, 6853−6863.

(21) Cohanoschi, I.; Yao, S.; Belfield, K. D.; Hernández, F. E. Effect of the concentration of organic dyes on their surface plasmon enhanced two-photon absorption cross section using activated Au nanoparticles. *J. Appl. Phys.* **2007**, *101*, 086112.

(22) Sivapalan, S. T.; Vella, J. H.; Yang, T. K.; Dalton, M. J.; Swiger, R. N.; Haley, J. E.; Cooper, T. M.; Urbas, A. M.; Tan, L.-S.; Murphy, C. J. Plasmonic Enhancement of the Two Photon Absorption Cross Section of an Organic Chromophore Using Polyelectrolyte-Coated Gold Nanorods. *Langmuir* **2012**, *28*, 9147−9154.

(23) Zhao, T.; Yu, K.; Li, L.; Zhang, T.; Guan, Z.; Gao, N.; Yuan, P.; Li, S.; Yao, S. Q.; Xu, Q.-H.; Xu, G. Q. Gold Nanorod Enhanced Two-Photon Excitation Fluorescence of Photosensitizers for Two-Photon Imaging and Photodynamic Therapy. *ACS Appl. Mater. Interfaces* **2014**, *6*, 2700−2708.

(24) Craciun, A. M.; Focsan, M.; Gaina, L.; Astilean, S. Enhanced one- and two-photon excited fluorescence of cationic (phenothiazinyl)vinyl-pyridinium chromophore attached to polyelectrolyte-coated gold nanorods. *Dyes Pigm.* **2017**, *136*, 24−30.

(25) Sivapalan, S. T.; Vella, J. H.; Yang, T. K.; Dalton, M. J.; Haley, J. E.; Cooper, T. M.; Urbas, A. M.; Tan, L.-S.; Murphy, C. J. Off-Resonant Two-Photon Absorption Cross-Section Enhancement of an Organic Chromophore on Gold Nanorods. *J. Phys. Chem. Lett.* **2013**, *4*, 749−752.

(26) Zhang, T.; Lu, G.; Liu, J.; Shen, H.; Perriat, P.; Martini, M.; Tillement, O.; Gong, Q. Strong two-photon fluorescence enhanced jointly by dipolar and quadrupolar modes of a single plasmonic nanostructure. *Appl. Phys. Lett.* **2012**, *101*, 051109.

(27) Gong, S.-H.; Kim, S.; Kim, J.-H.; Cho, J.-H.; Cho, Y.-H. Site-Selective, Two-Photon Plasmonic Nanofocusing on a Single Quantum

Dot for Near-Room-Temperature Operation. *ACS Photonics* **2018**, *5*, 711−717.
(28) Taylor, A. B.; Siddiquee, A. M.; Chon, J. W. M. Below Melting Point Photothermal Reshaping of Single Gold Nanorods Driven by Surface Diffusion. *ACS Nano* **2014**, *8*, 12071−12079.
(29) Zijlstra, P.; Chon, J. W.; Gu, M. White light scattering spectroscopy and electron microscopy of laser induced melting in single gold nanorods. *Phys. Chem. Chem. Phys.* **2009**, *11*, 5915−5921.
(30) Albrecht, W.; Deng, T.-S.; Goris, B.; van Huis, M. A.; Bals, S.; van Blaaderen, A. Single Particle Deformation and Analysis of Silica-Coated Gold Nanorods before and after Femtosecond Laser Pulse Excitation. *Nano Lett.* **2016**, *16*, 1818−1825.
(31) Link, S.; El-Sayed, M. A. Spectral Properties and Relaxation Dynamics of Surface Plasmon Electronic Oscillations in Gold and Silver Nanodots and Nanorods. *J. Phys. Chem. B* **1999**, *103*, 8410−8426.
(32) Zhang, K.; Chang, H.; Fu, A.; Alivisatos, A. P.; Yang, H. Continuous Distribution of Emission States from Single CdSe/ZnS Quantum Dots. *Nano Lett.* **2006**, *6*, 843−847.
(33) Talbot, C. B.; Patalay, R.; Munro, I.; Warren, S.; Ratto, F.; Matteini, P.; Pini, R.; Breunig, H. G.; Konig, K.; Chu, A. C.; Stamp, G. W.; Neil, M. A.; French, P. M.; Dunsby, C. Application of ultrafast gold luminescence to measuring the instrument response function for multispectral multiphoton fluorescence lifetime imaging. *Opt. Express* **2011**, *19*, 13848−61.
(34) Kinkhabwala, A. A.; Yu, Z.; Fan, S.; Moerner, W. E. Fluorescence correlation spectroscopy at high concentrations using gold bowtie nanoantennas. *Chem. Phys.* **2012**, *406*, 3−8.
(35) Khatua, S.; Yuan, H.; Orrit, M. Enhanced-fluorescence correlation spectroscopy at micro-molar dye concentration around a single gold nanorod. *Phys. Chem. Chem. Phys.* **2015**, *17*, 21127−21132.
(36) Galland, C.; Ghosh, Y.; Steinbrück, A.; Sykora, M.; Hollingsworth, J. A.; Klimov, V. I.; Htoon, H. Two types of luminescence blinking revealed by spectroelectrochemistry of single quantum dots. *Nature* **2011**, *479*, 203.
(37) Galland, C.; Ghosh, Y.; Steinbrück, A.; Hollingsworth, J. A.; Htoon, H.; Klimov, V. I. Lifetime blinking in nonblinking nanocrystal quantum dots. *Nat. Commun.* **2012**, *3*, 908.
(38) Ma, X.; Tan, H.; Kipp, T.; Mews, A. Fluorescence Enhancement, Blinking Suppression, and Gray States of Individual Semiconductor Nanocrystals Close to Gold Nanoparticles. *Nano Lett.* **2010**, *10*, 4166−4174.
(39) LeBlanc, S. J.; McClanahan, M. R.; Jones, M.; Moyer, P. J. Enhancement of multiphoton emission from single CdSe quantum dots coupled to gold films. *Nano Lett.* **2013**, *13*, 1662−1669.
(40) Yao, J.; Larson, D. R.; Vishwasrao, H. D.; Zipfel, W. R.; Webb, W. W. Blinking and nonradiant dark fraction of water-soluble quantum dots in aqueous solution. *Proc. Natl. Acad. Sci. U. S. A.* **2005**, *102*, 14284−14289.
(41) Caldarola, M.; Pradhan, B.; Orrit, M. Quantifying fluorescence enhancement for slowly diffusing single molecules in plasmonic near fields. *J. Chem. Phys.* **2018**, *148*, 123334.
(42) Biebricher, A.; Sauer, M.; Tinnefeld, P. Radiative and Nonradiative Rate Fluctuations of Single Colloidal Semiconductor Nanocrystals. *J. Phys. Chem. B* **2006**, *110*, 5174−5178.
(43) Amecke, N.; Cichos, F. Intermediate intensity levels during the emission intermittency of single CdSe/ZnS quantum dots. *J. Lumin.* **2011**, *131*, 375−378.
(44) Schlegel, G.; Bohnenberger, J.; Potapova, I.; Mews, A. Fluorescence decay time of single semiconductor nanocrystals. *Phys. Rev. Lett.* **2002**, *88*, 137401.
(45) Fisher, B. R.; Eisler, H.-J.; Stott, N. E.; Bawendi, M. G. Emission Intensity Dependence and Single-Exponential Behavior In Single Colloidal Quantum Dot Fluorescence Lifetimes. *J. Phys. Chem. B* **2004**, *108*, 143−148.
(46) He, G. S.; Yong, K.-T.; Zheng, Q.; Sahoo, Y.; Baev, A.; Ryasnyanskiy, A. I.; Prasad, P. N. Multi-photon excitation properties of CdSe quantum dots solutions and optical limiting behavior in infrared range. *Opt. Express* **2007**, *15*, 12818−12833.
(47) Yorulmaz, M.; Khatua, S.; Zijlstra, P.; Gaiduk, A.; Orrit, M. Luminescence quantum yield of single gold nanorods. *Nano Lett.* **2012**, *12*, 4385−91.
(48) Johnson, P. B.; Christy, R.-W. Optical constants of the noble metals. *Phys. Rev. B* **1972**, *6*, 4370.
(49) Homer Reid, M. T.; Johnson, S. G. Efficient Computation of Power, Force, and Torque in BEM Scattering Calculations. *ArXiv e-prints*, 2013.
(50) http://homerreid.com/scuff-EM.
(51) Novotny, L.; Hecht, B. *Principles of Nano-optics*; Cambridge University Press, 2012.

DOI: 10.1021/acsphotonics.8b00306
ACS Photonics 2018, 5, 2960−2968